ACS APPLIED MATERIALS & INTERFACES

Research Article

www.acsami.org

Indium Tin Oxide-Free Tandem Polymer Solar Cells on Opaque Substrates with Top Illumination

Dhritiman Gupta,*[,†,‡] Martijn M. Wienk,[‡] and René A. J. Janssen*[,‡]

[†]Materials innovation institute (M2i), 2600 GA Delft, Netherlands

[‡]Molecular Materials and Nanosystems, Eindhoven University of Technology, 5600 MB Eindhoven, Netherlands

Supporting Information

ABSTRACT: Top-illuminated, indium tin oxide (ITO)-free, tandem polymer solar cells are fabricated on opaque substrates in an inverted device configuration. In the tandem cell, a wide band gap subcell, consisting of poly[*N*-9′-heptadecanyl-2,7-carbazole-*alt*-5,5-(4′,7′-di-2-thienyl-2′,1′,3′-benzothiadiazole)] (PCDTBT) blended with [70]PCBM is combined with a small band gap subcell consisting of a mixture of poly[{2,5-bis(2-hexyldecyl)-2,3,5,6-tetrahydro-3,6-dioxopyrrolo[3,4-*c*]-pyrrole-1,4-diyl}-*alt*-{[2,2′-(1,4-phenylene)bisthiophene]-5,5′-diyl}] (PDPPTPT) and [60]PCBM. Compared to the more common bottom-illuminated inverted tandem polymer solar cells on transparent ITO substrates, the front and back cells must be reversed when using opaque substrates and a transparent and conductive top contact must be employed to enable top illumination. A high conductive poly(3,4-ethylenedioxythiophene):poly(styrenesulfonate) (PEDOT:PSS) layer in combination with Ag lines surrounding the active area as current collection electrode is used for this purpose. The tandem polymer solar cell on an opaque glass/metal substrate yields a power conversion efficiency of 6.1% when the thicknesses of the photoactive layers are balanced for optimum performance. This is similar to the equivalent inverted tandem device fabricated on a transparent glass/ITO substrate.

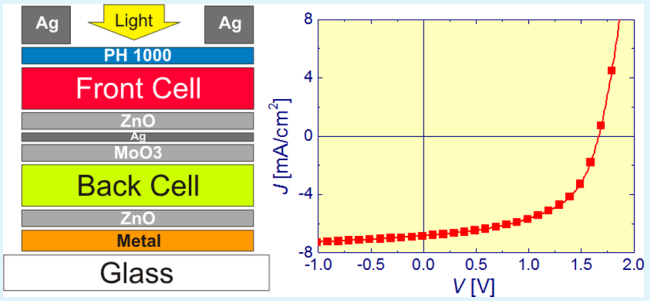

KEYWORDS: *conducting polymers, electrodes, tandem solar cell, opaque substrate, top illumination*

1. INTRODUCTION

In recent years, the power conversion efficiency (PCE) of single junction polymer solar cells has reached about 9%.[1−5] In most of the high efficiency polymer solar cells, the active layer consists of a small band gap polymer, suitably designed to capture a significant part of the high-energy and low-energy photons of the solar spectrum. While this strategy yields high current densities, the devices suffer from a low open-circuit voltage due to the thermalization of high-energy photons to the small band gap. In a series-connected tandem solar cell, a wide band gap polymer subcell is employed to compensate for the voltage loss and a small band gap polymer subcell, having a complementary red-shifted absorption profile, compensates for the transmission loss. This strategy affords both a high open-circuit voltage and broad spectral response. Recently, research in tandem polymer solar cells has attracted considerable interest and PCEs over 10%[6−8] have been reported. Research efforts in this field are concentrated on strategies to achieve higher efficiency, which includes proper material design,[9,10] designing efficient intermediate charge recombination layers,[11,12] and using inverted device geometry for enhanced light absorption and increased stability.[7,8,13]

For tandem polymer solar cells, two device configurations are commonly used.[6−9] In the inverted geometry, the tandem cell is built on top of an electron collection layer (ECL) as opposed to the regular geometry where it is built on top of a hole collection layer (HCL). In both cases, a transparent (glass/indium tin oxide (ITO)) substrate enables the light to enter through the substrate. This scheme of illumination is usually referred to as the superstrate configuration (Figure 1) and contrasts with a configuration in which the substrate is nontransparent. In this layout, called substrate configuration, illumination is from the top side and light does not pass the substrate (Figure 1). So far, ITO-free monolithic organic tandem solar cells have been demonstrated on transparent substrates only. Chen et al. have reported a transparent tandem cell on a glass/ITO substrate which can be illuminated from either side (Figure 1).[14]

Optically opaque substrates, like steel foils, are particularly interesting because of their mechanical robustness, their excellent barrier properties, and their thermal and chemical stability. An energy-generating functional coating on steel can be an effective way to integrate solar cells in packaging and building-integrated applications. Solar cells fabricated on steel can also find interesting applications in artificial leaves, where the substrate itself can act as an electrode.[15] To this end, we recently demonstrated ITO-free single junction polymer solar cells on steel substrates using a laminated high conductivity poly(3,4-ethylenedioxythiophene):poly(styrenesulfonate) (PE-

Received: May 28, 2014
Accepted: July 22, 2014
Published: July 22, 2014

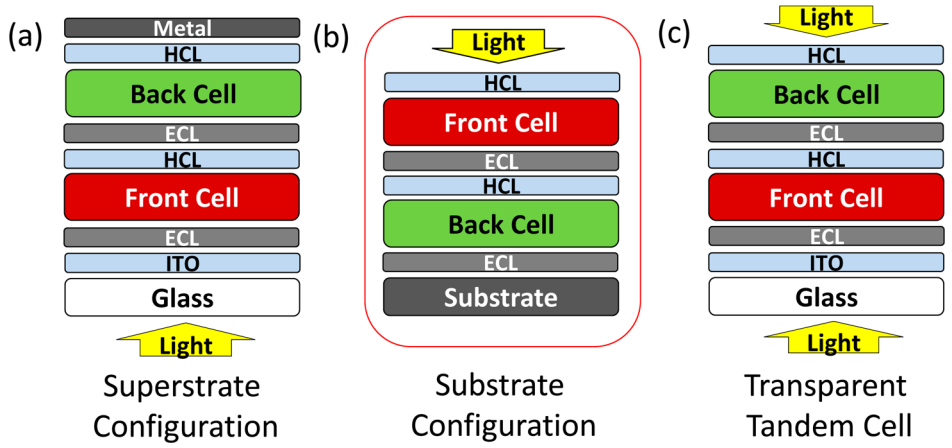

Figure 1. Three different schemes of illumination for an inverted geometry tandem solar cell. (a) In the superstrate configuration, light enters the device from substrate side. (b) In the substrate configuration, light enters the device from top side. (c) For a transparent solar cell, the device can be illuminated from either side.

DOT:PSS) layer as a transparent conducting top electrode.[16] In combination with an Ag contact surrounding the active area, the high conductivity PEDOT:PSS was found to form an efficient transparent and conducting electrode without any substantial optical, resistive, or voltage losses. For polymer solar cells that use such opaque substrates, we found that a device configuration in which the device stack is built on a primary layer of ZnO as ECL gives higher efficiency and is easier to fabricate than the reversed device layout in which a primary layer of PEDOT:PSS was used as HCL. This is similar to the approach followed by Inganäs et al. for inverted solar cells on an opaque Al/TiO_x bottom contact modified with an amphiphilic conjugated polymer interlayer and a high conductive PEDOT:PSS top contact.[17]

In this paper, we demonstrate an efficient ITO-free tandem solar cell fabricated on an optically opaque substrate. The tandem cells are fabricated on metal coated glass substrates in an inverted geometry, i.e., with a ZnO ECL as the first layer in the stack, and are compared with equivalent inverted devices fabricated on glass/ITO substrates. For the active layers, we use a small band gap diketopyrrolopyrrole polymer poly[{2,5-bis(2-hexyldecyl)-2,3,5,6-tetrahydro-3,6-dioxopyrrolo[3,4-*c*]pyrrole-1,4-diyl}-*alt*-{[2,2′-(1,4-phenylene)bisthiophene]-5,5′-diyl}] (PDPPTPT) (Figure 2) (E_g = 1.53 eV) blended with [60]PCBM in combination with a wide band gap layer consisting of poly[*N*-9′-heptadecanyl-2,7-carbazole-*alt*-5,5-(4′,7′-di-2-thienyl-2′,1′,3′-benzothiadiazole)] (PCDTBT) (Figure 2) (E_g = 1.88 eV) mixed with [70]PCBM. PDPPTPT and PCDTBT were chosen because of their complementary absorption spectra and high open-circuit voltages up to 0.9 and 0.8 V with PCBM, respectively. By using commercially available high conductivity PEDOT:PSS (Clevios PH1000) as the top electrode, tandem solar cells with PCE = 6.1% have been fabricated on opaque substrates. This efficiency is similar to that of the corresponding inverted tandem cell on a transparent substrate.

2. EXPERIMENTAL SECTION

2.1. Materials. Chromium (99.995%, Sigma-Aldrich), silver (99.99%, Sigma-Aldrich), gold (99.999%, Cerac), and molybdenum-(VI) oxide (99.99%, Sigma-Aldrich) for evaporation were used as received. Two different formulations of PEDOT:PSS were used: highly conductive Clevios PH1000 (solid content 1−1.3%) and low conductive Clevios P VP Al4083 (solid content 1.3−1.7%), both

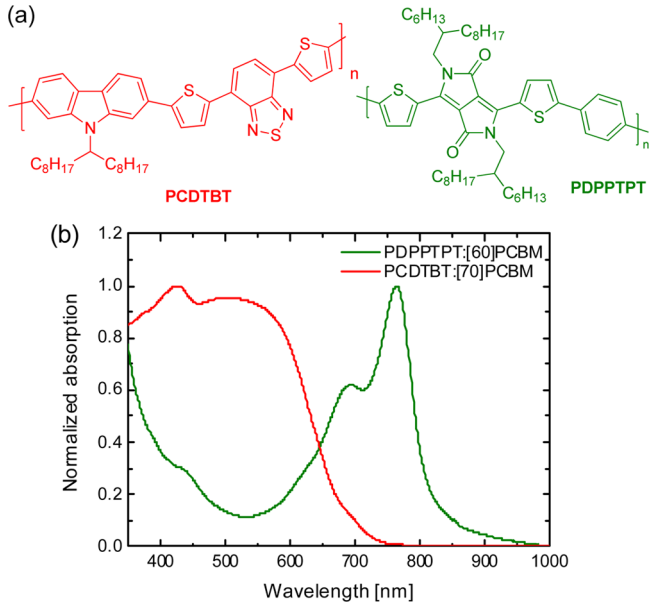

Figure 2. (a) Molecular structures of PCDTBT and PDPPTPT. (b) Normalized absorption spectra of PCDTBT:[70]PCBM and PDPPTPT: [60]PCBM blend films.

from Heraeus. Before use, 5 wt % dimethyl sulfoxide (DMSO) was added to PH1000 and the mixture was sonicated for 1 h and exhibited a conductivity of ∼900 S cm^{-1}. PH1000 was filtered using 5.0 μm (Whatman Puradisc FP30) filters, and for Clevios P VP Al4083 PEDOT, a 0.45 μm PVDF filter (Acrodisc LC) was used. To enable spin coating onto a hydrophobic polymer surface, fluorosurfactant Zonyl FS-300 (40% solid content in water) was added in both the PEDOT:PSS versions. To the PH1000/DMSO mixture, 0.2 wt % Zonyl was added. In Clevios P VP Al4083, 0.3 wt % Zonyl was added and the mixture was sonicated for 1 h. Poly[*N*-9′-heptadecanyl-2,7-carbazole-*alt*-5,5-(4′,7′-di-2-thienyl-2′,1′,3′-benzothiadiazole)] PCDTBT (1-material), [60]PCBM (>99%, Solenne BV), [70]PCBM (90−95%, Solenne BV), zinc acetate dihydrate (98%, Acros), 2-methoxyethanol (anhydrous 99.8%, Sigma-Aldrich), ethanolamine (99%, Sigma-Aldrich), chloroform, ortho-dichlorobenzene, and chlorobenzene ($CHCl_3$, ODCB, and CB 99%, Sigma-Aldrich) were used as received. ZnO nanoparticles (average diameter ∼5 nm, 10 mg mL^{-1}) were dispersed in 2-propanol.[18]

2.2. Device Fabrication. Glass and glass/ITO substrates were cleaned by sonicating in acetone and soapy water followed by rinsing

with normal water and sonicating in 2-propanol for a few minutes. Cr (5 nm)/Au (100 nm) metal contacts were evaporated on glass using a shadow mask. Metal-coated substrates were further treated with N_2 plasma (0.6 mbar, 70 W, 10−15 min.) in a Diener Femto PCCE plasma cleaner. ITO substrates were treated with UV−ozone for 30 min.

Single junction devices were fabricated by first spin coating a layer of ZnO onto the substrates. A ZnO sol−gel ink was prepared by adding 2-methoxyethanol (1 mL) and ethanolamine (30 μL) to zinc acetate dihydrate (109 mg), and the mixture was stirred at room temperature for 1 h. This ink was directly spun on N_2-plasma treated glass/Cr/Au and UV−ozone treated glass/ITO substrates at 2000 rpm spin speed and was subsequently annealed at 150 °C in air to yield a 64 nm thick film. The ZnO layer was not patterned, since the sheet resistance even after UV photodoping was found to be quite high (≈20 MΩ/square).

PCDTBT:[70]PCBM solutions were prepared by dissolving PCDTBT and [70]PCBM in a 1:4 weight ratio in CB at a polymer concentration of 7 mg mL^{-1} and stirring overnight at 70 °C. The mixture was spin coated inside a nitrogen filled glovebox at 1000 rpm spin speed to achieve a 120 nm thickness. The polymer solution was kept at 60 °C inside a glovebox, and spin coating was done from hot solution. For PCDTBT:[70]PCBM cells, low-conductivity PEDOT:PSS (Clevios P VP Al4083 + 0.3 wt % Zonyl) was spin coated at 3000 rpm on top of the active layer, and then, 100 nm of Ag was evaporated to complete the device. PCDTBT:[70]PCBM single junction devices were annealed at 70 °C for 10 min before UV exposure.

The PDPPTPT:[60]PCBM (1:2 w/w) solutions were prepared with a polymer concentration of 5 mg mL^{-1} in a mixture of ODCB and $CHCl_3$ (70 mg of ODCB in 1 mL of $CHCl_3$) and stirring at 70 °C for 1 h. Spin coating of the polymer solution was done inside a glovebox from a solution at room temperature and at a spin speed of 2000 rpm to create a 105 nm thick layer. After spin coating, the PDPPTPT:[60]PCBM cells were transferred to a thermal evaporation chamber where 10 nm of MoO_3 and 100 nm of Ag were deposited.

For the tandem devices on a glass/ITO substrate, a PCDTBT:[70]PCBM layer was spin coated on the ZnO ECL using identical processing conditions as for the single junction cells. On top of the PCDTBT:[70]PCBM layer, a layer (40 nm) of low conductivity PEDOT:PSS (Clevios P VP Al4083 + 0.3 wt % Zonyl) was spin coated at 3000 rpm outside the glovebox. The substrates were then transferred to a glovebox, where ZnO nanoparticle dispersion (10 mg mL^{-1}) was spin coated at 2000 rpm into a 30 nm layer. Next, the PDPPTPT:[60]PCBM layer was spin coated. Finally, 10 nm of MoO_3 as HCL and 100 nm of Ag were evaporated to complete the device. Substrates were not annealed at any stage. When attempting to replace the MoO_3 HCL with a spin coated PEDOT:PSS HCL, the cells exhibited electrical shorts between the two PEDOT:PSS layers.[13] The lateral conductivity of PEDOT:PSS enhances the effects of occasional shorts anywhere on the substrate. The low lateral conductivity of MoO_3 eliminates this problem. The tandem devices and PDPPTPT single junction devices were not annealed at any stage.

For devices fabricated on opaque substrates, 5 nm of Cr and 100 nm thick Au were evaporated on the glass substrates and acted as current collecting electrode. The square shaped Au electrode (areas of 0.09 cm^2 and 0.16 cm^2) defined the device area (Supporting Information, Figure S1). Then, a ZnO layer was deposited from a ZnO sol−gel ink as described for single junction cells. After spin coating the PDPPTPT:[60]PCBM layer, the substrates were transferred to the metal evaporator to deposit 10 nm of MoO_3 and 1 nm of Ag. Substrates were subsequently transferred inside a glovebox (without exposing to air) where a ZnO nanoparticle layer and a PCDTBT:[70]PCBM layer (from hot solution kept at 60 °C) were spin coated. For the top contact, PEDOT:PSS (Clevios PH1000) was mixed with 5 wt % DMSO to increase the conductivity and with 0.2 wt % Zonyl to enable spin coating on the hydrophobic photoactive layer. This PEDOT:PSS mixture was spin coated outside the glovebox at a spin speed of 1000 rpm for 3 min, followed by 5000 rpm for 30 s to dry the film. No annealing was done at any stage. Devices were completed by evaporating 100 nm thick Ag lines surrounding the bottom gold electrode through a shadow mask.

2.3. Measurements. Before all the measurements, the devices were illuminated with UV light for 2 min to photodope ZnO and increase its conductivity.[19] EQE measurements were performed in a home-built setup, with the devices kept in a nitrogen filled box with a quartz window and illuminated through an aperture of 2 mm diameter. Mechanically modulated (Chopper, Stanford Research, SR 540) monochromatic (Monochromator, Oriel, Cornerstone 130) light from a 50 W tungsten halogen lamp (Osram 64610) was used as probe light, in combination with continuous bias light from a solid state laser (B&W Tek Inc., 532 nm, 30 mW and Newport 505B, 830 nm, 30 mW). The intensity of the bias laser was adjusted using a variable-neutral density filter. A calibrated Si photodiode was used for measuring the reference spectrum. The response was recorded as the voltage over a 50 Ω resistance, using a lock-in amplifier (Stanford Research Systems, SR830). For measuring the spectral response of each subcell of the tandem cell, bias light is essential. A 530 nm laser provided bias light for the PCDTBT:[70]PCBM subcell, while a 830 nm laser was used to bias the PDPPTPT:[60]PCBM subcell. In combination with light bias, a compensating electrical bias corresponding to the V_{OC} of the concerned subcell was applied by the lock-in amplifier to ensure short circuit conditions in the respective subcells.

Current density vs voltage curves ($J-V$) were measured under simulated solar light (100 mW cm^{-2}, from a tungsten−halogen lamp filtered by a Schott GG385 UV filter and a Hoya LB120 daylight filter) using a Keithley 2400 source meter. No mismatch correction was done. For the single junction cells, the accurate short-circuit current density (J_{SC}) was determined from the EQE by integrating with the AM1.5G solar spectrum.[20] For the tandem solar cell measurement, the simulated solar light spectrum was tuned to provide appropriate illumination to each subcell. This was done by adjusting the voltage applied to the tungsten halogen lamp in such a way that both the wide band gap and the small band gap single junction cells gave the same J_{SC} as determined from the EQE measurement. The $J-V$ curves of the tandem solar cell on ITO substrate were measured under illumination through a mask (mask area 0.0676 cm^2, actual device area 0.09 cm^2) to avoid the extra current contribution due to the lateral conductivity of Clevios P VP Al4083 PEDOT:PSS. During characterizing the tandem devices fabricated on glass/metal substrate, we observed current fluctuations (Supporting Information, Figure S2) that implied resistive switching, which is commonly seen in metal oxide based diodes.[21,22] This feature was particularly pronounced in the fourth quadrant. However, after sweeping the device in the dark with a large applied voltage (typically −6 to +6 V), a smooth $J-V$ response was recorded. Thicknesses of all different layers was measured using a Veeco Dektak 150 Surface Profiler.

2.4. Optical Simulations. To determine the optimum thicknesses for each subcell in the tandem, the following procedure was used. First, a series of single junction solar cells was fabricated with different active layer thicknesses using optimized processing conditions. The wide band gap single junction cell had the following configuration, ITO/ZnO/PCDTBT:[70]PCBM/PEDOT:PSS/Ag, and the small band gap cell had the configuration: ITO/ZnO/PDPPTPT:[60]PCBM/MoO_3/Ag. For each thickness of the active layer, $J-V$ curves were measured under simulated AM1.5G white light illumination and internal quantum efficiencies were determined (Supporting Information, Figure S3). Using a commercial software package (SETFOS 3, Fluxim AG), the number of photons absorbed in the two photoactive layers in the whole stack of the tandem device was determined for AM1.5G solar illumination. Using the experimentally determined IQE for each thickness as input allows one to determine the current generated in each subcell. Combining the current generation in each subcell with the relevant shape of the $J-V$ curve and adding the $J-V$s of each subcell for a combination of thicknesses for front and back subcells, the $J-V$ curve of the tandem device is obtained. For the tandem device on the opaque substrate, we used parameters of the same single junction cells, fabricated on glass/ITO. The tandem stack was changed accordingly in the SETFOS simulation. The refractive index (n) and

extinction coefficient (k) were either measured or taken from the literature.[16,19,23]

3. RESULTS AND DISCUSSION

3.1. Single Junction Cells. To create a tandem cell, both small and wide band gap cells have to work in concert and be optimized for best performance. The small band gap polymer, PDPPTPT, used in this study was initially shown to yield PCE = 5.5% in single junction cells.[24] Recent progress improved the molecular weight of this polymer, which resulted in an increased PCE = 7% in combination with [70]PCBM in a regular device configuration.[25] In the tandem cells, we use PDPPTPT in combination with [60]PCBM instead of [70]PCBM, to reduce adverse absorption of high-energy photons in the small band gap active layer. Single junction PDPPTPT:[60]PCBM solar cells in an inverted configuration on glass substrates with ITO/ZnO bottom and MoO_3/Ag top electrodes were fabricated as described in the Experimental Section. The current density−voltage (J−V) characteristics and external quantum efficiency (EQE) of the optimized solar cells are shown in Figure 3, and the performance parameters are summarized in Table 1. For a 105 nm thick active layer, a 6.1% PCE and 58% maximum EQE (at λ = 700 nm) were obtained.

For the wide band gap subcell, a blend of PCDTBT and [70]PCBM is used. PCDTBT is one of the best performing wide band gap polymers[26,27] and was previously used to demonstrate 7% efficient tandem cells.[23] The PCDTBT:[70]PCBM layer was deposited on glass/ITO/ZnO and covered with PEDOT:PSS (Clevios P VP Al4083) as described in the Experimental Section. Spin coating of the water based PEDOT:PSS dispersion on top of the hydrophobic polymer−fullerene surface requires either modification of polymer surface energy, e.g., by plasma treatment,[13] or the use of additives to improve the wettability of the aqueous PEDOT:PSS dispersion on the photoactive layer. We used a fluorosurfactant (0.3 wt % Zonyl FS300). The J−V characteristics and the EQE values are shown in Figure 3, and the performance parameters are summarized in Table 1. Single junction devices with a 120 nm thick PCDTBT:[70]PCBM active layer, yielded PCE = 3.7% and maximum EQE = 58% (at λ = 480 nm). The difference observed between J_{SC} measured under white light and that obtained from integrating EQE spectra (Table 1) is due to the fact that the white-light source contains less blue light.

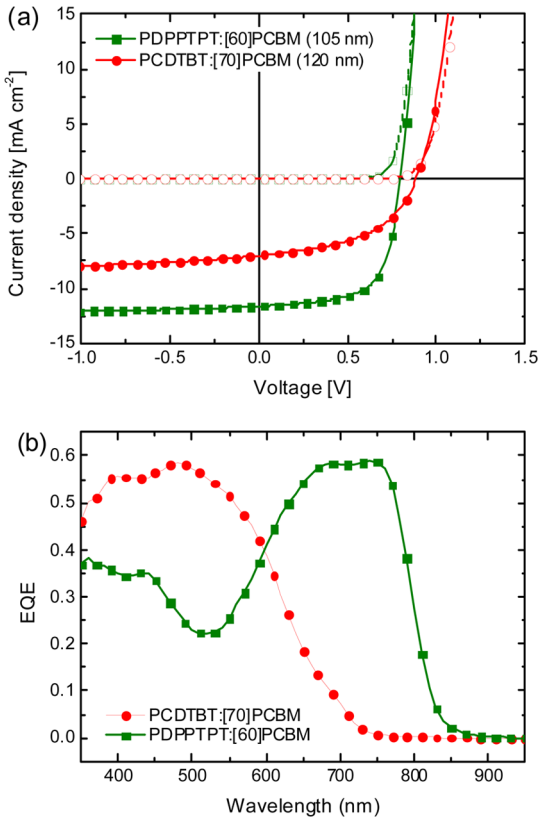

Figure 3. (a) J−V characteristics of the optimized single junction solar cells under simulated AM1.5G illumination. Device configuration of the wide band gap cell: ITO/ZnO/PCDTBT:[70]PCBM/PEDOT:PSS/Ag; configuration of the small band gap cell: ITO/ZnO/PDPPTPT:[60]PCBM/MoO_3/Ag. (b) EQE spectra of the same cells.

Table 1. Photovoltaic Parameters for Single Junction Inverted Cells

active layer	J_{SC}[a] [mA cm^{-2}]	J_{SC}[b] [mA cm^{-2}]	V_{OC} [V]	FF	PCE [%]
PCDTBT:[70]PCBM	7.0	8.4	0.89	0.49	3.7
PDPPTPT:[60]PCBM	12.2	11.6	0.80	0.66	6.1

[a]Determined from white light J−V. [b]Determined from integrating EQE spectra with the AM1.5G spectrum. EQE spectra are acquired without bias light illumination.

We note that a small amount of Zonyl (0.1 wt %) has been shown to improve the sheet resistance of highly-conductive PEDOT:PSS (PH1000).[28] The combination has previously been used as a replacement for ITO in P3HT:PCBM based solar cells without affecting the V_{OC} of the device.[28] For PCDTBT:[70]PCBM devices, however, we observed a loss in V_{OC} (~100 mV) in combination with Clevios P VP Al4083 PEDOT:PSS but not with PH1000 PEDOT:PSS. Postannealing (after deposition of the Ag back electrode) on these devices helps to restore the major part of this loss.

3.2. Tandem Junction Cells. Inverted tandem polymer solar cells were first fabricated on ITO coated glass substrates in the superstrate device configuration: ITO/ZnO/PCDTBT:[70]PCBM/PEDOT:PSS/ZnO/PDPPTPT:[60]PCBM/MoO_3/Ag (Figure 4a) as described in the Experimental Section. Optical simulations revealed that the most advantageous tandem configuration is the one where the wide band gap cell is the front cell and the small band gap cell the back cell. For determining the optimum layer thicknesses for the front and back cells, optical modeling was performed using the SETFOS 3 simulation tool combined with the experimentally determined internal quantum efficiencies (IQE) (Supporting Information, Figure S3) and the normalized shape of the J−V curves determined for a range of different layer thickness of both active layers as described in detail in ref 29. Using the optical constants and electrical characteristics of the subcells, the performance of the tandem cell can be predicted by combining the J−V curves of representative single junction cells under the lighting conditions experienced in the tandem cell.[29] The predicted photovoltaic parameters (J_{SC}, V_{OC}, FF, and PCE) for the tandem cell as a function of front cell and back cell thicknesses are shown in the Supporting Information (Figure S4). The highest performance in the tandem is predicted for front cells with a thickness in the range of 80 to 120 nm and back cells with thickness in the range of 70 to 100 nm.

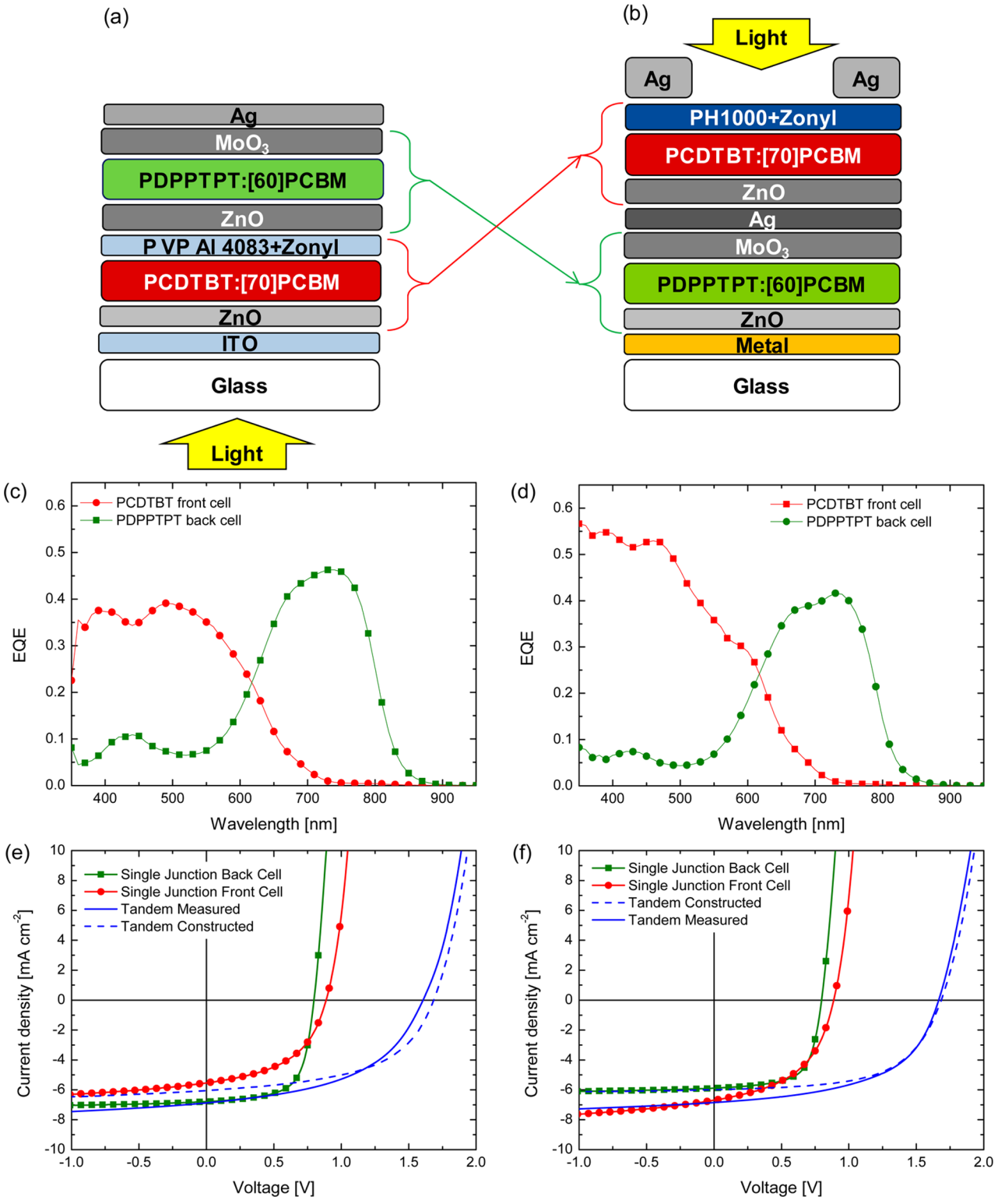

Figure 4. Tandem device configuration on (a) transparent glass/ITO substrate and (b) on opaque glass/metal substrate. On the glass/metal substrate, the sequence of the subcells is reversed as shown with the arrows because light enters now from the top side. EQE spectra measured under appropriate light and an electrical bias condition for tandem device on (c) glass/ITO and (d) glass/metal substrates. *J*–*V* characteristics of the single junction cells measured under appropriate reduced light intensity and the mathematically constructed *J*–*V* characteristics of the tandem (dotted line). The solid line depicts the measured *J*–*V* response for tandem devices on (e) glass/ITO and on (f) glass/metal substrates.

The EQE and the *J*–*V* characteristics of inverted tandem devices on glass/ITO with a 120 nm PCDTBT:[70]PCBM front cell and a 105 nm PDPPTPT:[60]PCBM back cell are shown in Figure 4c,e. The EQE of the tandem cell was measured under appropriate light and electrical bias conditions to obtain the EQE response of each subcell under short circuit condition.[30] The EQE of each subcell was multiplied with the AM1.5G (100 mW cm^{-2}) solar spectrum and integrated over

dx.doi.org/10.1021/am503262e | *ACS Appl. Mater. Interfaces* 2014, 6, 13937−13944

the whole spectral range to obtain the short circuit current (J_{SC}) generated in each subcell. Using this procedure, J_{SC} = 5.54 mA cm^{-2} was measured for the PCDTBT:[70]PCBM subcell and J_{SC} = 6.79 mA cm^{-2} for the PDPPTPT:[60]PCBM subcell. The $J-V$ curves of the corresponding single junction cells were measured simultaneously under a properly adjusted white light source. The intensity of the white light source was adjusted such that the J_{SC} of the single junction cells matches with the J_{SC} of the subcells in the tandem device. Assuming a loss free intermediate contact, the $J-V$ curve of the tandem can then be constructed by adding the $J-V$s of the two single-junction cells.[31] We refer to this as the mathematically constructed $J-V$ curve; it provides some information on the extra losses created in the tandem, compared to the sum of the single junctions. The measured and mathematically constructed tandem $J-V$s are shown in Figure 4e, and parameters are summarized in Table 2, including the results from the predicting simulations

Table 2. Summary of Performance Parameters for Tandem Solar Cell

substrate	device	J_{SC} [mA cm^{-2}]	V_{OC} [V]	FF	PCE [%]
transparent	tandem measured	6.88[a]	1.61	0.49	5.4
	tandem simulated	6.89	1.67	0.56	6.4
	tandem mathematically constructed	6.06[b]	1.68	0.53	5.4
	wide band gap subcell	5.54[b]			
	small band gap subcell	6.79[b]			
opaque	tandem measured	6.85[a]	1.67	0.54	6.1
	tandem simulated	6.72	1.67	0.55	6.2
	tandem mathematically constructed	6.01[b]	1.68	0.60	6.0
	wide band gap subcell	6.70[b]			
	small band gap subcell	5.89[b]			

[a]Measured with adjusted white light intensity (100 mW cm^{-2}) tuned to the specific spectral sensitivities of the sub cells. [b]Based on EQE.

(Supporting Information, Figures S4 and S5). The measurements on the tandem device yield PCE = 5.4%, with V_{OC} = 1.61 V and FF = 0.49 (the average PCE over four nominally identical cells was 5.2%). Comparison with the parameters of the mathematically constructed $J-V$ curves (V_{OC} = 1.68 V and FF = 0.53) reveals a loss of 70 mV in V_{OC} and a loss in FF, indicative of significant losses in the intermediate ZnO/PEDOT:PSS recombination layer. The predicted J_{SC} = 6.89 mA cm^{-2} value from the simulated $J-V$ response (Table 2 and see the Supporting Information, Figure S5) matches well with the J_{SC} = 6.88 mA cm^{-2} measured with the adjusted white light, but the predicted FF = 0.56 and V_{OC} = 1.67 are again higher and show a closer match with the constructed $J-V$. With a recombination contact that is free from resistive and voltage losses, a 6.4% PCE would be expected (Table 2).

To fabricate tandem devices on an opaque substrate, the location of the wide and small band gap subcells in the device stack must be interchanged (Figure 4a,b), because light now enters the device from the top and not through the substrate. The rearrangement ensures maximum absorption of high-energy photons in the wide band gap and of low-energy photons in the small band gap subcells when the device is illuminated from the top. Devices were fabricated on chromium/gold (Cr/Au) coated glass substrates. The recombination layer in between the PDPPTPT:[60]PCBM and PCDTBT:[70]PCBM photoactive layers comprises two metal oxide layers, namely, 10 nm of thermally evaporated MoO_3 and 30 nm of ZnO layer, spin coated from a nanoparticle dispersion. Both MoO_3[32] and ZnO are n-type materials and therefore electron−hole recombination will occur at the MoO_3/PDPPTPT interface. In order to increase the ohmicity of the MoO_3/ZnO recombination contact, a 1 nm thin layer of thermally deposited Ag is introduced between two oxide layers.[33−35] As the top electrode, high conductivity PEDOT:PSS and an Ag electrode surrounding the active area were used (Experimental Section).

Like for the transparent substrates, we evaluated the effect of varying thickness of the two photoactive layers for the opaque substrate with top illumination using combined optical and electrical modeling[29] (Supporting Information, Figure S6). On the basis of these simulations, PCEs in excess of 6% are expected for front cells with thicknesses in the range of 80 to 120 nm and back cells with thicknesses in the range of 70 to 105 nm. Tandem cells on opaque glass/Au substrates were made with a front cell of 120 nm and a back cell of 105 nm. EQE measurements on the tandem device were performed as described above to yield the J_{SC} of the respective subcells. Interestingly and in contrast to the glass/ITO based inverted tandem cells, J_{SC} = 6.70 mA cm^{-2} for the PCDTBT:[70]PCBM front cell, slightly higher than the J_{SC} = 5.89 mA cm^{-2} measured for the PDPPTPT:[60]PCBM back cell (Figure 4d). This difference possibly originates from a slight underestimation of the EQE and the integrated J_{SC} of the glass/ITO based tandem. The EQE was measured with optical and electrical bias. Because the V_{OC} of the glass/ITO tandem is 70 mV less than the sum of the subcell V_{OC}'s, the bias voltage that must be used cannot be accurately determined. By using the V_{OC} of the other subcell, the EQE is then measured in the fourth quadrant instead of at short circuit and hence reduced. This effect is particularly significant in the PCDBT:[70]PCBM subcell.

$J-V$ characteristics measured under adjusted white light illumination corresponding to AM1.5G reveal PCE = 6.1% for the opaque tandem cell (the average PCE over six nominally identical cells was 5.8%). The experimentally measured $J-V$ response matches well with the one predicted from simulations (Table 2 and the Supporting Information, Figures S5 and S6). The experimental V_{OC} of 1.67 V implies a negligible voltage loss at the metal oxide based recombination contact. The FF = 0.54 measured for the tandem cell is lower than the FF (= 0.60) found by mathematically constructing the $J-V$ curve of the single junction reference cells but close to the value of FF = 0.55 predicted from the simulations (Table 2). Nevertheless, the FF of the tandem cell on an opaque glass/Au substrate is somewhat improved over its counterpart fabricated on glass/ITO substrates. This improvement could originate from the better current matching obtained between the subcells, which is evident from the $J-V$ curves (Figure 4f). Recently, Lassiter et al. have pointed out that the FF of the tandem follows the FF of the current limiting cell. In the present case, there is an advantageous situation where the current limiting cell has the highest FF.[36] The J_{SC} measured in these tandems is similar to that measured in the tandems on glass/ITO substrate. This indicates that, optically, both the tandem structures are equivalent.

As can be seen in Table 2, the measured, simulated, and constructed values for J_{SC} of both tandem cells are not exactly equal; the latter is somewhat smaller for both the transparent

and opaque substrates. This is possibly a result of an underestimation of the EQE of the subscells but also demonstrates the challenges encountered in determining these values accurately for tandem cells.

4. CONCLUSION

In conclusion, we have demonstrated that tandem devices can be successfully fabricated on optically opaque substrates with efficiencies when illuminated from the top that are similar to that of the corresponding inverted tandem cell on a transparent substrate. The tandem device fabricated in an inverted structure has a low loss recombination contact based on two metal oxides where charge recombination is mediated by a thin Ag layer and uses a high conductivity PEDOT:PSS (PH1000) as a transparent hole charge collection layer and a Ag line surrounding the active area as the top electrode. Measured photovoltaic parameters match closely with those predicted from optical modeling. The efficiency of the tandem device (PCE = 6.1%) is mainly limited by the wide band gap cell which yields low internal quantum efficiency and a low FF, particularly at larger active layer thicknesses. These results demonstrate that tandem polymer solar cells with highly reflective metal back contacts can be a viable route to efficient photovoltaic devices on opaque substrates.

■ ASSOCIATED CONTENT

Supporting Information

Device contact pad layouts, current fluctuation observed in tandem solar cell $J-V$ made on opaque substrates, internal quantum efficiencies of wide band gap and small band gap single junction cells, SETFOS simulation results for tandem cells on glass/ITO and glass/metal substrates, and comparison of simulated and measured tandem solar cell parameters. This material is available free of charge via the Internet at http://pubs.acs.org.

■ AUTHOR INFORMATION

Corresponding Authors

*E-mail: r.a.j.janssen@tue.nl. Fax: +31-40-2451036. Tel: +31-40-2473597.

*E-mail: d.gupta@tue.nl.

Notes

The authors declare no competing financial interest.

■ ACKNOWLEDGMENTS

We thank Serkan Esiner and Alice Furlan for useful discussions. This research was carried out under project number M71.3.10406 in the framework of the Research Program of the Materials innovation institute M2i.

■ REFERENCES

(1) Green, M. A.; Emery, K.; Hishikawa, Y.; Warta, W.; Dunlop, E. D. Solar Cell Efficiency Tables (Version 41). *Prog. Photovoltaics* **2013**, *21*, 1−11.

(2) Dou, L.; Chang, W.-H.; Gao, J.; Chen, C.-C.; You, J.; You Yang, Y. A Selenium-Substituted Low-Bandgap Polymer with Versatile Photovoltaic Applications. *Adv. Mater.* **2013**, *25*, 825−831.

(3) Dou, L.; Gao, J.; Richard, E.; You, J.; Chen, C.-C.; Cha, K. C.; He, Y.; Li, G.; Yang, Y. Systematic Investigation of Benzodithiophene- and Diketopyrrolopyrrole-Based Low-Bandgap Polymers Designed for Single Junction and Tandem Polymer Solar Cells. *J. Am. Chem. Soc.* **2012**, *134*, 10071−10079.

(4) He, Z.; Zhong, C.; Su, S.; Xu, M.; Wu, H.; Cao, Y. Enhanced Power-Conversion Efficiency in Polymer Solar Cells Using an Inverted Device Structure. *Nat. Photonics* **2012**, *6*, 591−595.

(5) Cabanetos, C.; Labban, A. E.; Bartelt, J. A.; Douglas, J. D.; Mateker, W. R.; Fréchet, J. M. J.; McGehee, M. D.; Beaujuge, P. M. Linear Side Chains in Benzo[1,2-b:4,5-b′]dithiophene−Thieno[3,4-c]pyrrole-4,6-dione Polymers Direct Self-Assembly and Solar Cell Performance. *J. Am. Chem. Soc.* **2013**, *135*, 4656−4659.

(6) Ameri, T.; Lia, N.; Brabec, C. J. Highly Efficient Organic Tandem Solar Cells: A Follow up Review. *Energy Environ. Sci.* **2013**, *6*, 2390−2413.

(7) You, J.; Dou, L.; Yoshimura, K.; Kato, T.; Ohya, K.; Moriartry, T.; Emery, K.; Chen, C.-C.; Gao, J.; Li, G.; Yang, Y. A Polymer Tandem Solar Cell with 10.6% Power Conversion Efficiency. *Nat. Commun.* **2013**, *4*, 1446.

(8) You, J.; Chen, C.-C.; Hong, Z.; Yoshimura, K.; Ohya, K.; Xu, R.; Ye, S.; Gao, J.; Li, G.; Yang, Y. 10.2% Power Conversion Efficiency Polymer Tandem Solar Cells Consisting of Two Identical Sub-Cells. *Adv. Mater.* **2013**, *25*, 3973−3978.

(9) Li, W.; Furlan, A.; Hendriks, K. H.; Wienk, M. M.; Janssen, R. A. J. Efficient Tandem and Triple-Junction Polymer Solar Cells. *J. Am. Chem. Soc.* **2013**, *135*, 5529−5532.

(10) Kim, J.-H.; Song, C. E.; Kim, H. U.; Grimsdale, A. C.; Moon, S.-J.; Shin, W. S.; Choi, S. K.; Hwang, D.-H. High Open Circuit Voltage Solution-Processed Tandem Organic Photovoltaic Cells Employing a Bottom Cell Using a New Medium Band Gap Semiconducting Polymer. *Chem. Mater.* **2013**, *25*, 2722−2732.

(11) Li, N.; Baran, D.; Forberich, K.; Turbiez, M.; Ameri, T.; Krebs, F. C.; Brabec, C. J. An Efficient Solution-Processed Intermediate Layer for Facilitating Fabrication of Organic Multi-Junction Solar Cells. *Adv. Energy Mater.* **2013**, *3*, 1597−1605.

(12) Zhou, Y.; Fuentes-Hernandez, C.; Shim, J. W.; Khan, T. M.; Kippelen, B. High Performance Polymeric Charge Recombination Layer for Organic Tandem Solar Cells. *Energy Environ. Sci.* **2012**, *5*, 9827−9832.

(13) Kouijzer, S.; Esiner, S.; Frijters, C. H.; Turbiez, M.; Wienk, M. M.; Janssen, R. A. J. Efficient Inverted Tandem Polymer Solar Cells with a Solution-Processed Recombination Layer. *Adv. Energy Mater.* **2012**, *2*, 945−949.

(14) Chen, C.-C.; Dou, L.; Gao, J.; Chang, W.-H.; Li, G.; Yang, Y. High-Performance Semi-Transparent Polymer Solar Cells Possessing Tandem Structures. *Energy Environ. Sci.* **2013**, *6*, 2714−2720.

(15) Reece, S. Y.; Hamel, J. A.; Sung, K.; Jarvi, T. D.; Esswein, A. J.; Pijpers, J. J. H.; Nocera, D. G. Wireless Solar Water Splitting Using Silicon-Based Semiconductors and Earth-Abundant Catalysts. *Science* **2011**, *334*, 645−648.

(16) Gupta, D.; Wienk, M. M.; Janssen, R. A. J. Efficient Polymer Solar Cells on Opaque Substrates with a Laminated PEDOT:PSS Top Electrode. *Adv. Energy Mater.* **2013**, *3*, 782−787.

(17) Tang, Z.; Andersson, L. M.; George, Z.; Vandewal, K.; Tvingstedt, K.; Hendriksson, P.; Kroon, R.; Andersson, M. R.; Inganäs, O. Interlayer for Modified Cathode in Highly Efficient Inverted ITO-Free Organic Solar Cells. *Adv. Mater.* **2012**, *24*, 554−558.

(18) Beek, W. J. E.; Wienk, M. M.; Kemerink, M.; Yang, X.; Janssen, R. A. J. Hybrid Zinc Oxide Conjugated Polymer Bulk Heterojunction Solar Cells. *J. Phys. Chem. B* **2005**, *109*, 9505−9516.

(19) Lakhwani, G.; Roijmans, R. F. H.; Kronemeijer, A. J.; Gilot, J.; Janssen, R. A. J.; Meskers, S. C. J. Probing Charge Carrier Density in a Layer of Photodoped ZnO Nanoparticles by Spectroscopic Ellipsometry. *J. Phys. Chem. C* **2010**, *114*, 14804−14810.

(20) Wienk, M. M.; Turbiez, M.; Gilot, J.; Janssen, R. A. J. Narrow-Bandgap Diketo-Pyrrolo-Pyrrole Polymer Solar Cells: The Effect of Processing on the Performance. *Adv. Mater.* **2008**, *20*, 2556−2560.

(21) Verbakel, F.; Meskers, S. C. J.; de Leeuw, D. M.; Janssen, R. A. J. Resistive Switching in Organic Memories with a Spin-Coated Metal Oxide Nanoparticle Layer. *J. Phys. Chem. C* **2008**, *112*, 5254−5257.

(22) Verbakel, F.; Meskers, S. C. J.; Janssen, R. A. J.; Gomes, H. L.; van den Biggelaar, A. J. M.; de Leeuw, D. M. Switching Dynamics in Non-Volatile Polymer Memories. *Org. Electron.* **2008**, *9*, 829−833.
(23) Gevaerts, V. S.; Furlan, A.; Wienk, M. M.; Turbiez, M.; Janssen, R. A. J. Solution Processed Polymer Tandem Solar Cell Using Efficient Small and Wide Bandgap Polymer:Fullerene Blends. *Adv. Mater.* **2012**, *24*, 2130−2134.
(24) Bijleveld, J. C.; Gevaerts, V. S.; Nuzzo, D. D.; Turbiez, M.; Mathijssen, S. G. J.; de Leeuw, D. M.; Wienk, M. M.; Janssen, R. A. J. Efficient Solar Cells Based on an Easily Accessible Diketopyrrolopyrrole Polymer. *Adv. Mater.* **2010**, *22*, E242−E246.
(25) Hendriks, K. H.; Heintges, G. H. L.; Gevaerts, V. S.; Wienk, M. M.; Janssen, R. A. J. High-Molecular-Weight Regular Alternating Diketopyrrolopyrrole-based Terpolymers for Efficient Organic Solar Cells. *Angew. Chem., Int. Ed.* **2013**, *52*, 8341−8344.
(26) Blouin, N.; Michaud, A.; Leclerc, M. A Low-Bandgap Poly(2,7-Carbazole) Derivative for Use in High-Performance Solar Cells. *Adv. Mater.* **2007**, *19*, 2295−2300.
(27) Chu, T.-Y.; Alem, S.; Verly, P. G.; Wakim, S.; Lu, J.; Tao, Y.; Beaupré, S.; Leclerc, M.; Bélanger, F.; Désilets, D.; Rodman, S.; Waller, D.; Gaudiana, R. Highly Efficient Polycarbazole-Based Organic Photovoltaic Devices. *Appl. Phys. Lett.* **2009**, *95*, 063304.
(28) Vosgueritchian, M.; Lipomi, D. J.; Bao, Z. Highly Conductive and Transparent PEDOT:PSS Films with a Fluorosurfactant for Stretchable and Flexible Transparent Electrodes. *Adv. Funct. Mater.* **2012**, *22*, 421−428.
(29) Gilot, J.; Wienk, M. M.; Janssen, R. A. J. Optimizing Polymer Tandem Solar Cells. *Adv. Mater.* **2010**, *22*, E67−E71.
(30) Gilot, J.; Wienk, M. M.; Janssen, R. A. J. Measuring the External Quantum Efficiency of Two-Terminal Polymer Tandem Solar Cells. *Adv. Funct. Mater.* **2010**, *20*, 3904−3911.
(31) Hadipour, A.; de Boer, B.; Blom, P. W. M. Device Operation of Organic Tandem Solar Cells. *Org. Electron.* **2008**, *9*, 617−624.
(32) Greiner, M. T.; Helander, M. G.; Tang, W.-M.; Wang, Z.-B.; Qiu, J.; Lu, Z.-H. Universal Energy-Level Alignment of Molecules on Metal Oxides. *Nat. Mater.* **2012**, *11*, 76−81.
(33) Yakimov, A.; Forrest, S. R. High Photovoltage Multiple-Heterojunction Organic Solar Cells Incorporating Interfacial Metallic Nanoclusters. *Appl. Phys. Lett.* **2002**, *80*, 1667−1669.
(34) Chou, C.-H.; Kwan, W. L.; Hong, Z.; Chen, L.-M.; Yang, Y. A Metal-Oxide Interconnection Layer for Polymer Tandem Solar Cells with an Inverted Architecture. *Adv. Mater.* **2011**, *23*, 1282−1286.
(35) Puetz, A.; Steiner, F.; Mescher, J.; Reinhard, M.; Christ, N.; Kutsarov, D.; Kalt, H.; Lemmer, U.; Colsmann, A. Solution Processable, Precursor Based Zinc Oxide Buffer Layers for 4.5% Efficient Organic Tandem Solar Cells. *Org. Electron.* **2012**, *13*, 2696−2701.
(36) Lassiter, B. E.; Renshaw, C. K.; Forrest, S. R. Understanding Tandem Organic Photovoltaic Cell Performance. *J. Appl. Phys.* **2013**, *113*, 214505.